Fermi National Accelerator Laboratory

FERMILAB-Conf-95/106-E

DØ

Observation of the Top Quark

Joey Thompson
For the DØ Collaboration

University of Maryland
College Park, Maryland 20742

Fermi National Accelerator Laboratory
P.O. Box 500, Batavia, Illinois 60510

May 1995

Presented at the XXXth *Rencontres de Moriond, QCD and High Energy Hadronic Interactions,*
Les Arcs, France, March 19-26, 1995

Operated by Universities Research Association Inc. under Contract No. DE-AC02-76CHO3000 with the United States Department of Energy

Disclaimer

OBSERVATION OF THE TOP QUARK

Joey Thompson
University of Maryland
College Park, MD 20742

for

The DØ Collaboration

Abstract

The DØ collaboration reports on a search for the Standard Model top quark in $p\bar{p}$ collisions at $\sqrt{s} = 1.8$ TeV at the Fermilab Tevatron, with an integrated luminosity of approximately 50 pb^{-1}. We have searched for $t\bar{t}$ production in the dilepton and single-lepton decay channels, with and without tagging of b quark jets. We observe 17 events with an expected background of 3.8 ± 0.6 events. The probability for an upward fluctuation of the background to produce the observed signal is 2×10^{-6} (equivalent to 4.6 standard deviations). The kinematic properties of the excess events are consistent with top quark decay. We conclude that we have observed the top quark and measure its mass to be 199^{+19}_{-21} (stat.) ± 22 (syst.) GeV/c^2 and its production cross section to be 6.4 ± 2.2 pb.

1 Introduction

The Standard Model requires that the b quark have a weak isospin partner, the hitherto unobserved top quark. The search for the top quark and the measurement of its properties are an important test of the Standard Model. Certain Standard Model parameters, including m_W, m_Z, $\sin^2\theta_W$, and Z boson decay asymmetries depend on the top quark mass, and to a lesser extent on the Higgs boson mass, through radiative corrections involving top quark loops. Precision measurements of these parameters permit an indirect measurement of the top quark mass which can be compared to that obtained by direct measurement. These precision measurements currently suggest a top quark mass in the range 150–210 GeV/c^2 [1].

The most sensitive searches for the Standard Model top quark have been carried out at the Fermilab Tevatron by the DØ and CDF experiments. Recent results from these experiments based on data from the 1992–1993 Tevatron run (run Ia) include a lower limit on m_t of 131 GeV/c^2 by DØ [2], a 2.8σ positive result by CDF [3], and a 1.9σ positive result by DØ [4].

In this article, we assume that the top quark is pair-produced and decays 100% of the time into a W boson and a b quark. The search is divided into seven distinct channels depending on how the two W bosons decay, and on whether or not a soft muon from a b or c quark semileptonic decay is observed. The so-called dilepton channels occur when both W bosons decay leptonically ($e\mu$ + jets, ee + jets, and $\mu\mu$ + jets). The single-lepton channels occur when just one W boson decays leptonically (e + jets and μ + jets). The single-lepton channels are subdivided into b-tagged and untagged channels according to whether or not a muon is observed consistent with $b \to \mu + X$. The muon-tagged channels are denoted e + jets/μ and μ + jets/μ. The data set for this analysis includes data from run Ia and run Ib with an integrated luminosity of about 50pb^{-1} with slight differences among the seven channels. The new results reported here from DØ [6] and CDF [5] based on new data from the ongoing 1994–1995 Tevatron run (run Ib) increase the significance of the top quark signal to $> 4\sigma$ for each experiment.

2 Particle Detection

The DØ detector and data collection systems are described elsewhere [7].

Muons are detected and momentum-analyzed using an iron toroid spectrometer located outside of a uranium-liquid argon calorimeter and a non-magnetic central tracking system inside the calorimeter. Muons are identified by their ability to penetrate the calorimeter and the spectrometer magnet yoke. Two distinct types of muons are defined. "High-p_T" muons, which are predominantly from gauge boson decay, are required to be isolated from jet axes by distance $\Delta\mathcal{R} > 0.5$ in η-ϕ space (η = pseudorapidity = $\tanh^{-1}(\cos\theta)$; θ, ϕ = polar, azimuthal angle), and to have transverse momentum $p_T > 12$ GeV/c. "Soft" muons, which are primarily from b, c or π/K decay, are required to be within distance $\Delta\mathcal{R} < 0.5$ of any jet axis. The minimum p_T for soft muons is 4 GeV/c. The maximum η for both kinds of muons is 1.7 for run Ia data and 1.0 for run Ib data. The η restriction is tightened for run Ib data due to forward muon chamber aging.

Electrons are identified by their longitudinal and transverse shower profile in the calorimeter and are required to have a matching track in the central tracking chambers. The background

from photon conversions is suppressed by an ionization (dE/dx) criterion on the chamber track. A transition radiation detector is used to confirm the identity of electrons for $|\eta| < 1$. Electrons are required to have $|\eta| < 2.5$ and transverse energy $E_T > 15$ GeV.

Jets are reconstructed using a cone algorithm of radius $\mathcal{R} = 0.5$.

The presence of neutrinos in the final state is inferred from missing transverse energy ($\not\!\!E_T$). The calorimeter-only $\not\!\!E_T$ ($\not\!\!E_T^{\rm cal}$) is determined from energy deposition in the calorimeter for $|\eta| < 4.5$. Correcting $\not\!\!E_T^{\rm cal}$ for the measured p_T of detected muons yields the total $\not\!\!E_T$.

3 The Counting Experiment

The event selection for this analysis is chosen to give maximum expected significance for top quark masses of 180–200 GeV/c^2, using the ISAJET event generator [8] to model the top quark signal (assuming the calculated Standard Model top quark pair production cross section [9]), and using our standard background estimates as described below. In this analysis, we achieve a signal-to-background ratio of 1:1 for a top quark mass of 200 GeV/c^2. This is a better signal-to-background ratio, but with smaller acceptance, than our previously published analyses [2, 4]. The improved rejection arises primarily by requiring events to have a larger total transverse energy by means of a cut on a quantity we call H_T. H_T is defined as the scalar sum of the E_T's of the jets (for the single-lepton and $\mu\mu$ + jets channels), or the scalar sum of the E_T's of the leading electron and the jets (for the $e\mu$ + jets and ee + jets channels). In addition to the "standard" event selection, a "loose" selection is defined which does not include an H_T cut. This is done as a consistency check and to provide a less biased event sample for the top quark mass analysis.

The signature for the dilepton channels is defined as two isolated leptons, two or more jets, and large $\not\!\!E_T$. The signature for the single-lepton channels is defined as one isolated lepton, large $\not\!\!E_T$, and three or more jets (with muon tag) or four or more jets (without tag). The single-lepton signature includes either a soft muon tag or a "topological tag," based on H_T and the aplanarity of the jets $\mathcal{A}$, which is proportional to the smallest eigenvalue of the momentum tensor of the jets in the laboratory. "Double-tagged" events are counted only once, as part of the muon tagged channels. A summary of the kinematic cuts can be found in Table 1.

Additional special cuts are used in the ee + jets, $\mu\mu$ + jets and μ + jets/μ channels to remove background from Z + jets. To remove $Z \rightarrow ee$ background in ee + jets, we require that $|m_{ee} - m_Z| > 12$ GeV/c^2, or $\not\!\!E_T^{\rm cal} > 40$ GeV. To remove background from $Z \rightarrow \mu\mu$, the event as a whole is required to be inconsistent with Z + jets based on a global kinematic fit. The loose event selection cuts differ from those listed in Table 1 by the removal of the H_T requirement and by the relaxation of the aplanarity requirement for e + jets and μ + jets from $\mathcal{A} > 0.05$ to $\mathcal{A} > 0.03$. These loose cuts result in a factor of approximately five increase in predicted background.

H_T is a powerful discriminator between background and high-mass top quark production. Figure 1 shows a comparison of the shapes of the H_T distributions expected from background and 200 GeV/c^2 top quarks in the channels (a) $e\mu$ + jets and (b) untagged single-lepton + jets. The understanding of background H_T distributions is tested by comparing data and calculated

Table 1: Minimum kinematic requirements for the standard event selection (energy in GeV).

	High-p_T Leptons		Jets		Missing E_T		Muon Tag	Topological	
Channel	$E_T(e)$	$p_T(\mu)$	$N_{\rm jet}$	E_T(jet)	$\not\!\!E_T^{\rm cal}$	$\not\!\!E_T$	$p_T(\mu)$	H_T	$\mathcal{A}$
$e\mu$ + jets	15	12	2	15	20	10	-	120	-
ee + jets	20		2	15	25	-	-	120	-
$\mu\mu$ + jets		15	2	15	-	-	-	100	-
e + jets	20		4	15	25	-	-	200	0.05
μ + jets		15	4	15	20	20	-	200	0.05
e + jets/μ	20		3	20	20	-	4	140	-
μ + jets/μ		15	3	20	20	20	4	140	-

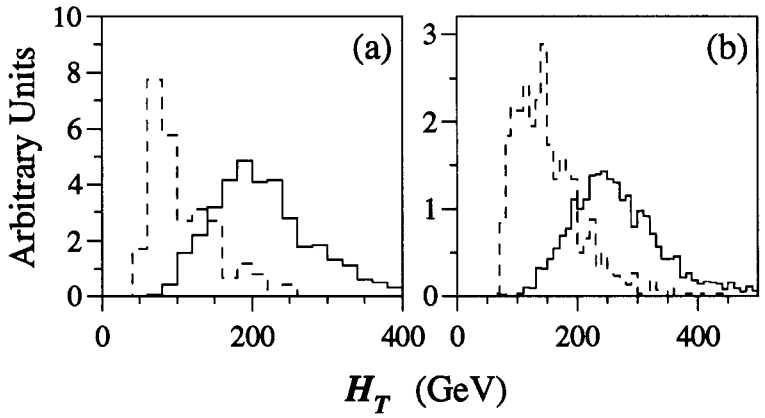

Figure 1: Shape of H_T distributions expected for the principal backgrounds (dashed line) and 200 GeV/c^2 top quarks (solid line) for (a) $e\mu$ + jets and (b) untagged single-lepton + jets.

background in background-dominated channels such as electron + $\not\!\!E_T$ + two jets and electron + $\not\!\!E_T$ + three jets [6]. The observed H_T distribution agrees with the background calculation, which includes contributions from both W + jets as calculated by the VECBOS Monte Carlo [10] and QCD multijet events.

The acceptance for $t\bar{t}$ events is calculated using the ISAJET event generator [8] and a detector simulation based on the GEANT program [11]. Differences in the acceptance found using the HERWIG event generator [12] are included in the systematic error.

Physics backgrounds (those having the same final state particles as the signal) were estimated using Monte Carlo simulation or a combination of Monte Carlo and data. The instrumental background from jets misidentified as electrons is estimated entirely from data using the measured jet misidentification probability (typically 2×10^{-4}). Other backgrounds for muons (*e.g.* hadronic punchthrough and cosmic rays) are found to be negligible for the signatures in question.

For the dilepton channels, the principle backgrounds are from Z and continuum Drell-Yan production ($Z, \gamma^* \rightarrow ee, \mu\mu$, and $\tau\tau$), vector boson pairs (WW, WZ), heavy flavor ($b\bar{b}$ and $c\bar{c}$)

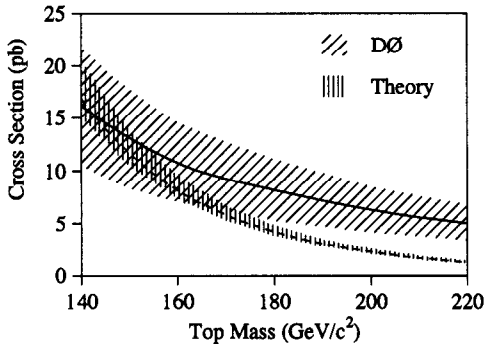

Figure 2: DØ measured $t\bar{t}$ production cross section (solid line with one standard deviation error band) as a function of assumed top quark mass. Also shown is the theoretical cross section curve (dashed line) [9].

production, and backgrounds with jets misidentified as leptons.

For the untagged single-lepton channels, the principle backgrounds are from W + jets, Z + jets, and multijet production with a jet misidentified as a lepton. The W + jets background is estimated using jet-scaling. In this method, we extrapolate the W + jets cross section from one and two jets, to four or more jets assuming an exponential dependence on the number of jets, as predicted by QCD [10], and as observed experimentally. The efficiency of the topological cuts for W + 4 jets is calculated using the VECBOS Monte Carlo program [10]. The QCD multijet background is determined independently from data using the measured jet fake probability. The Z + jets background is estimated by Monte Carlo calculation.

For the tagged single-lepton channels the observed jet multiplicity spectrum of untagged single lepton background events is convoluted with the measured tagging rate per jet to determine the total background. The tagging rate is observed to be a function of the number of jets in the event and the E_T's of the jets and is the same within error for both multijet and W + jets events. As a cross check, tagging-rate predictions were made for dijet, multijet, and gamma+jet samples and found to agree with the data.

From all seven channels, we observe 17 events with an expected background of 3.8 ± 0.6 events (see Table 2). Our measured cross section as a function of the top quark mass hypothesis is shown in Fig. 2. Assuming a top quark mass of 200 GeV/c^2, the production cross section is 6.3 ± 2.2 pb. The error in the cross section includes an overall 12% uncertainty in the luminosity. The probability of an upward fluctuation of the background to 17 or more events is 2×10^{-6}, which corresponds to 4.6 standard deviations for a Gaussian probability distribution. We have calculated the probability for our observed distribution of excess events among the seven channels and find that our results are consistent with top quark branching fractions at the 53% CL. A top production cross-section was calculated for the dilepton, tagged, and untagged single-lepton channels independently assuming the top hypothesis both for the "standard cuts" and "loose cuts." All agree within error. Thus, we observe a statistically significant excess of events, and the distribution of events among the seven channels is consistent with top quark production. We conclude that we have observed the top quark.

Additional confirmation that our observed excess contains a high-mass object comes from

Table 2: Summary of number of events observed, the predicted background, and the probability for the background to account for the data for both standard and loose cuts. A top quark pair production cross section is also given for an assumed top quark mass of 200 GeV/c^2.

	Standard Selection	Loose Selection
Dileptons	3	4
Lepton + Jets (Shape)	8	23
Lepton + Jets (Muon tag)	6	6
All channels	17	33
Background	3.8 ± 0.6	20.6 ± 3.2
Probability	2×10^{-6} (4.6σ)	0.023 (2.0σ)
$\sigma_{t\bar{t}}$ $(m_t = 200$ GeV/$c^2)$	6.3 ± 2.2 pb	4.5 ± 2.5 pb

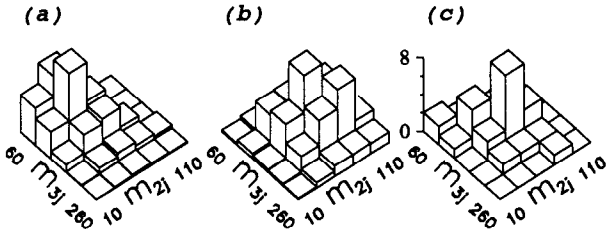

Figure 3: Single-lepton + jets two-jet *vs.* three-jet invariant mass distribution for (a) background, (b) 200 GeV/c^2 top Monte Carlo (ISAJET), and (c) data.

the invariant masses of jet combinations in single-lepton + jets events. For this analysis, single-lepton + four-jet events are selected using the loose event selection requirements (27 events). An invariant mass analysis is performed based on the hypothesis $t\bar{t} \rightarrow W^+W^-b\bar{b} \rightarrow \ell\nu q\bar{q}b\bar{b}$. One jet is assigned to the semileptonically decaying top quark and three jets are assigned to the hadronically decaying top quark. The jet assignment algorithm attempts to assign one of the two highest E_T jets to the semileptonically decaying top quark and to minimize the difference between the masses of the two top quarks. The invariant mass of the three jets assigned to the hadronically decaying top quark is denoted by m_{3j}. Among the three possible jet pairs from the hadronically decaying top quark, the smallest invariant mass is denoted by m_{2j}. Figure 3 shows the distribution of m_{3j} *vs.* m_{2j} for (a) background (W + jets and multijet) (b) 200 GeV/c^2 top Monte Carlo, and (c) data. The data are peaked at higher invariant mass, in both dimensions, than the background. Based only on the shapes of the distributions, the hypothesis that the data are a combination of top quark and background events (60% CL) is favored over the pure background hypothesis (3% CL).

4 Mass Analysis

We attempt to extract the top quark mass from our single-lepton + four-jet event sample using a 2-constraint kinematic fit to the hypothesis $t\bar{t} \rightarrow W^+W^-b\bar{b} \rightarrow \ell\nu q\bar{q}b\bar{b}$. Assignment of the

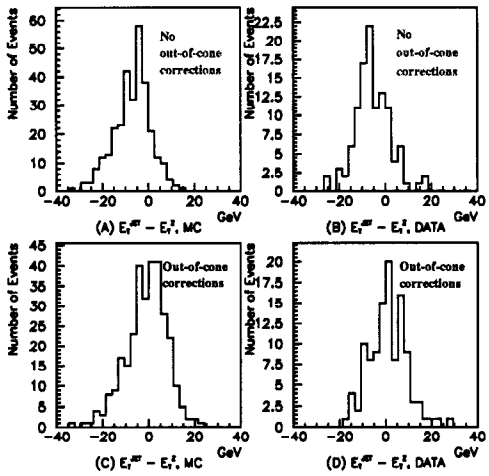

Figure 4: E_T balance in Z + jets events for Monte Carlo data, with and without parton level (out-of-cone) energy corrections.

four highest E_T jets to partons is made using a combinatoric algorithm.

We find that the chance of a successful solution of the combinatoric problem is greater using a narrower jet cone. We therefore use cone jets with radius $\mathcal{R} = 0.3$ for the mass determination as opposed to the $\mathcal{R} = 0.5$ cone jets which are used in the event selection for both the counting experiment and the mass analysis.

Correction of the measured energy inside the jet cone to the energy of the original parton takes place in two stages. The first stage, which is mainly data driven, is the correction of raw cone jets to idealized, detector-independent cone jets. The detector dependent corrections are for the calorimeter energy response, particle showering in and out of the cone in the calorimeter, and the subtraction of noise and energy from the underlying event. The second stage, which is a theoretical construct derived from Monte Carlo studies, is the correction of the idealized cone jet to the energy of the original parton. We test our jet energy corrections by examining the E_T balance in $Z(\rightarrow ee)+$jets events. We make a 1-constraint kinematic fit to the Z + jets hypothesis (like the top quark kinematic fit, but without mass constraints or jet assignment ambiguities). Figure 4 shows the E_T residuals for the jets resulting from this fit for Monte Carlo and data, with and without parton level jet energy corrections. If we compare the residuals with and without the parton energy corrections (Fig. 4(a),(b) *vs.* (c),(d)), we find a better accounting of the E_T balance (mean of distribution closer to zero) with parton energy corrections. We also see reasonable agreement between Monte Carlo and data (Fig. 4(a),(c) *vs.* (b),(d)) whether or not parton energy corrections are included.

In the ideal case where the four quarks give rise to four distinct jets, the number of possible solutions to the jet-parton assignment problem is twelve. In the case of a single b-tag the number of possible jet assignments is reduced to six. An additional twofold ambiguity arises from the two possible solutions for the longitudinal momentum of the neutrino produced by the leptonically decaying W boson. Actually, the amount of ambiguity in the mass-fitting problem is larger than suggested by the above naive combinatoric analysis. Effects such as gluon radiation and jets being lost due to merging or falling below energy thresholds make the correct solution more difficult, and sometimes impossible, to find. In cases where there are more than four jets,

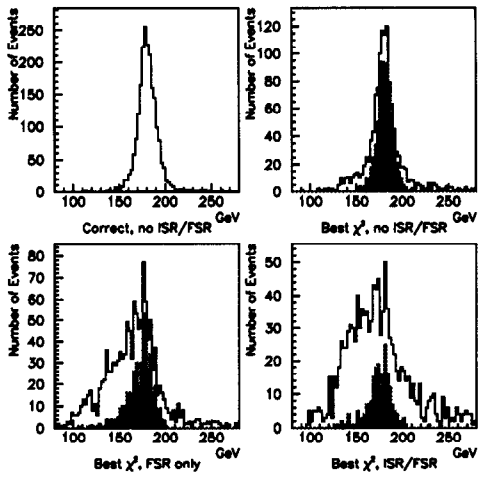

Figure 5: Effect of wrong combinations, initial and final state gluon radiation on top quark mass resolution for ISAJET Monte Carlo events with 180 GeV/c^2 top quark mass. The shaded areas of the histograms are what is obtained when Monte Carlo information is used to make the correct jet assignments in the presence of gluon radiation.

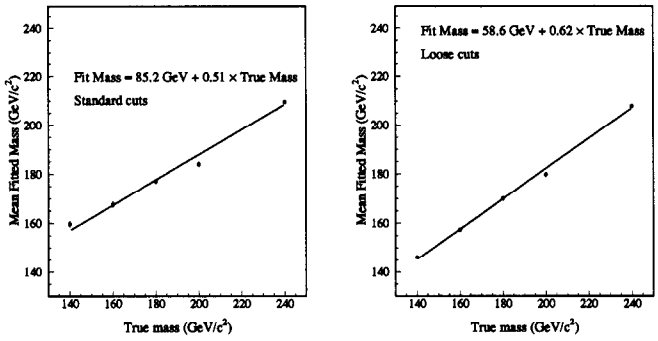

Figure 6: Mean value of fitted top quark mass *vs.* ISAJET input top quark mass for standard and loose selection criteria.

we use only the four highest E_T jets and ignore the rest. More sophisticated treatments of the fifth and higher number jets are found not to give any improvement in Monte Carlo studies. Rather than simply using the solution with the smallest χ^2, we use a χ^2-probability-weighted average top quark mass (with weight $e^{-\chi^2/2}$) from up to three solutions having $\chi^2 < 7$. The top quark mass resolution obtained in this way is found to be slightly better than that which is obtained from the smallest chisquare solution alone. The effects of wrong combinations, initial state gluon radiation (ISR), and final state gluon radiation (FSR) on the top quark mass resolution are shown in Fig. 5. We see from this figure that the combination of gluon radiation and combinatoric ambiguities together are much worse than either effect alone.

Despite the uncertainties and the difficulty in finding correct jet assignments, Monte Carlo studies show that the top quark mass obtained by kinematic fitting is strongly correlated with the input top quark mass. The relationship between the true (Monte Carlo) top quark mass and the mean fitted top quark mass is shown in Fig. 6.

An unbinned maximum likelihood fit is used to extract the top quark mass likelihood dis-

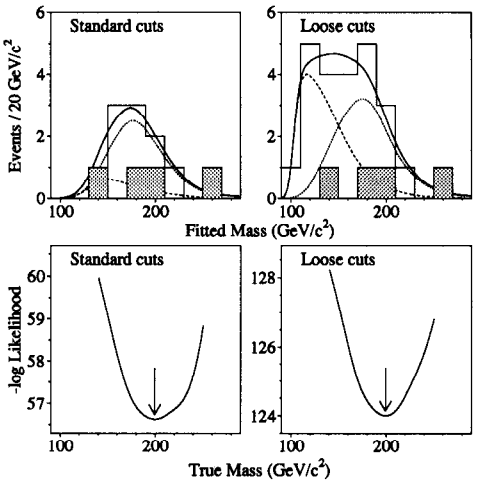

Figure 7: Fitted mass and mass likelihood distributions for standard and loose cuts. Shaded events have a soft muon tag.

tribution from a given sample of candidate events. The likelihood function used is given by:

$$L = e^{-(n_b-\langle n_b\rangle)^2/2\sigma^2}\frac{(n_s+n_b)^N}{N!}e^{-(n_s+n_b)}\prod_i \frac{n_s f_s(m_t,m_i)+n_b f_b(m_i)}{n_s+n_b} \quad (1)$$

The unknowns are the number of expected signal events n_s, the number of expected backgrounds n_b, and the top quark mass m_t. The inputs are the number of candidate events N, the fitted masses of the candidate events $m_i, (i = 1,\ldots,N)$, and the nominal background $\langle n_b\rangle$ and its error σ as determined in the counting experiment. The functions f_s and f_b are the expected distributions of fitted mass for signal and background. Both f_s and f_b are determined by Monte Carlo calculation and smoothed so that they are continuous functions of m_i and m_t. The likelihood function consists of three multiplicative factors representing a constraint on the background normalization, overall Poisson counting statistics, and the relative likelihood for each event to be a top quark event (for a given top quark mass) or background.

The entire mass determination machinery has been tested using Monte Carlo data. We have verified that mass bias of the kinematic fit is removed by the likelihood fit, and that the statistical error on the top quark mass from the likelihood fit scales inversely as the square root of the number of candidate events.

Eleven of the 14 single-lepton + four-jet candidate events selected using the standard cuts, and 24 of the 27 candidate events selected using the loose cuts, have successful kinematic fits. The kinematic fit can fail because there are fewer than four jets (in the case of b-tagged events), or because there are no solutions with good χ^2. The fitted mass and likelihood distributions of these events are shown in Fig. 7. The top quark mass extracted from the likelihood curve is 199^{+31}_{-25} (stat.) GeV/c^2 for standard cuts and 199^{+19}_{-21}(stat.) GeV/c^2 for loose cuts. The statistical errors are derived using $\Delta L = 0.5$. The result of the likelihood fit for the loose cuts sample does not change significantly if the background constraint is removed from the likelihood function. Because of its smaller error, we use the loose cuts mass determination as our official mass result.

The systematic error on the mass determination is dominated by the jet energy scale uncertainty which we estimate to be 10% or less. The top mass measurement depends on having an event generator that realistically models effects such as gluon radiation and jet shapes. Our

main result is based on ISAJET; repeating the measurement using HERWIG results in a 4 GeV/c^2 lower mass which we include in the systematic error. The total systematic error on the top quark mass is 22 GeV/c^2.

5 Conclusions

We have searched for top quark signals in seven channels in a data sample having an integrated luminosity of 50 pb^{-1}. We observe 17 candidate events with an expected background of 3.8 ± 0.6 events. The excess is statistically significant. The probability for the background to fluctuate up to 17 events is 2×10^{-6}, which corresponds to 4.6σ in the case of Gaussian errors. We measure the top quark mass to be 199^{+19}_{-21}(stat.) $\pm$ 22(syst.)GeV/c^2. Using the acceptance calculated at our central top quark mass, we measure the top quark pair production cross section to be $\sigma_{t\bar{t}} = 6.4 \pm 2.2$ pb.

References

[1] D. Schaile, CERN-PPE/94-162, presented at 27th International Conference on High Energy Physics, Glasgow, July 1994 (unpublished).

[2] DØ Collaboration, S. Abachi *et al.*, Phys. Rev. Lett. **72**, 2138 (1994).

[3] CDF Collaboration, F. Abe *et al.*, Phys. Rev. D **50**, 2966 (1994); Phys. Rev. Lett. **73**, 225 (1994).

[4] DØ Collaboration, S. Abachi *et al.*, Phys. Rev. Lett. bf 74, 2422 (1995).

[5] CDF Collaboration, F. Abe *et al.*, Phys. Rev. Lett. **74**, 2626 (1995).

[6] DØ Collaboration, S. Abachi *et al.*, Phys. Rev. Lett. bf 74, 2632 (1995).

[7] DØ Collaboration, S. Abachi *et al.*, Nucl. Instrum. Methods **A338**, 185 (1994).

[8] F. Paige and S. Protopopescu, BNL Report no. BNL38034, 1986 (unpublished), v6.49.

[9] E. Laenen, J. Smith, and W. van Neerven, Phys. Lett. **321B**, 254 (1994).

[10] F. Berends, H. Kuijf, B. Tausk, and W. Giele, Nucl. Phys. **B357**, 32 (1991).

[11] F. Carminati *et al.*, "GEANT Users Guide," CERN Program Library, December 1991 (unpublished).

[12] G. Marchesini *et al.*, Comput. Phys. Commun. **67**, 465, (1992).